PP/Elastomer/Filler Hybrids. II. Morphologies and Fracture

YU LONG* and ROBERT A. SHANKS

CRC for Polymer Blends, Applied Chemistry, Royal Melbourne Institute of Technology, Melbourne, Australia

SYNOPSIS

Three microstructures of polypropylene (PP)/elastomer/filler hybrids were obtained by processing control and elastomer or PP surface modification: (a) filler and elastomer particles are dispersed in a PP matrix to form separate particles; (b) elastomer particles with a filler core are distributed in a PP matrix; or (c) there are mixed microstructures of (a) and (b). Morphologies and fracture of different components and microstructures were studied by SEM. When the lower-temperature cut samples were carefully etched, the differences between the various microstructures were clearly observed under SEM. The core–shell microstructure provided an elastomer interlayer between the filler and the PP matrix, which resulted in changing the fracture mechanism from microcrack to shear yield. The SEM micrographs were digitized and analyzed by IMAGE 1.52. Rubber particle size and distribution were studied. The relationship between the morphologies and mechanical properties, especially the brittle–toughness transition, was discussed. DSC was used to confirm the difference of microstructures, crystallization behavior, and compatibility. © 1996 John Wiley & Sons, Inc.

INTRODUCTION

A study of processing, microstructure, and mechanical properties of three-component polypropylene (PP)/elastomer/filler hybrids was reported in a previous article.[1] Various microstructures of three-component PP/elastomer/filler systems could be obtained by the control of processing conditions and/or the chemical modification of PP or the elastomer: (a) Fillers and rubber particles are independently dispersed in the PP matrix to form a separated particle microstructure; (b) rubber particles with a filler core are distributed in the PP matrix to form a core–shell microstructure; or (c) there are mixed microstructures of (a) and (b). Mechanical properties of various three-component PP–elastomer–filler hybrids depended on different microstructures. For a certain PP–elastomer–filler system, a separated microstructure increased stiffness, while a core–shell microstructure improved toughness.

In this article, a detailed study of morphologies and fracture are reported. Various fillers (talc, $CaCO_3$, and nylon-12) and different maleic anhydride-modified elastomers [poly(ethylene-*co*-propylene), EP, and poly(styrene-*b*-ethylene-*co*-butylene-*b*-styrene), SEBS] were used in the experiments. The results of fresh impact fracture surfaces and cut surfaces by a microtome under −130°C are discussed. Rubber particle size and particle-size distribution were studied by digital image processing and analysis. DSC was used to identify the difference between the separated and core–shell microstructures and to study crystallization behavior and compatibility.

EXPERIMENTAL

Materials and Specimen Preparation

Different microstructures of PP/rubber/filler hybrids were obtained by processing control and polymer modification with maleic anhydride. To obtain separated microstructures, maleic anhydride-grafted PP (ma-PP) was mixed with EP and the filler using a Haake twin-screw extruder followed by granulation. Maleic anhydride-modified elastomers (ma-EP and ma-SEBS) were used to keep the filler particles inside the elastomer shell, thus producing a core–

* To whom correspondence should be addressed.

Journal of Applied Polymer Science, Vol. 62, 639–646 (1996)
 CCC 0021-8995/96/040639-08

shell microstructure. Alternatively, using processing control only, the filler and the unmodified elastomer were dispersed first, then the filler elastomer combination was dispersed in PP. This two-step dispersion method was also used with maleated elastomers to provide a greater degree of a core–shell microstructure. Standard test specimens were prepared using an injection-molding machine. Further details of the polymers and the blend preparation was described in a previous article.[1]

Surface Preparation

Undistorted and smooth surfaces were obtained by a Leica Reichert ultramicrotome, with a low-temperature chamber and glass knives. The operation conditions were the following: knife angle, 48°; knife temperature, −130°C; sample temperature, −130°C; and sample cross section, ~ 1 × 1 mm. The glass knife was quickly dulled in the low-temperature cutting operations, so a fresh length of knife edge was used to cut each surface. The cut surfaces were etched by xylene to selectively dissolve elastomer (EP or SEBS), leaving PP and talc undissolved. Surfaces were generally etched in xylene in a thermostatted ultrasonic bath at 20°C for 10 min.

The fresh impact fracture surface was obtained directly from impact testing at 20°C. Undeformed fracture surfaces were obtained through breaking specimens perpendicularly to the injection-molding direction after immersion of the specimens in liquid nitrogen for 20 min.

SEM Conditions

The surfaces were examined after they had been coated with a gold–palladium alloy using a JEOL JSM-840A SEM. To avoid distortion of the surface, the coating was applied for 10 s; then after a 10 s pause, the coating was repeated for a total of 100 s. Micrographs were obtained by collecting secondary electrons emitted upon bombarding the sample with 20 kV electrons. Micrographs were obtained at magnifications ranging from 1000 to 10,000. SEM micrographs were digitized, then analyzed by IMAGE 1.52. Rubber particle size and distribution were calculated.

Differential Scanning Calorimetry (DSC)

A Perkin-Elmer DSC7 was used to study the thermal behavior and microstructure. Measurements were made on approximately the same sample masses, which were cut from the surface of impact specimen bars with about 20 μm thickness. Melting temperature, T_m, and crystallization temperature, T_c, were obtained by heating and then cooling the sample at 20°C/min.

RESULTS AND DISCUSSION

In the PP/rubber/filler hybrids, the location of the filler is the key factor which controlled the morphologies. Different microstructures were obtained by controlling processing conditions and polymer surface modification.[1] Grafted maleic anhydride was used as a polar group to enhance the adhesion between the polymer and the mineral fillers. Maleic anhydride-grafted polymer was also used as a functional group to produce a chemical reaction with polyamide (PA, nylon-12) which was used as a meltable "filler." Separated particle microstructures were produced by introducing maleic anhydride-grafted PP in the matrix, while core–shell microstructures were obtained by introducing maleic anhydride-grafted elastomer.

The difference in the microstructures of PP/rubber/elastomer hybrids was observed from cut and etched surfaces. Figure 1 shows the surfaces cut by a microtome under −130°C and then etched by xylene in a thermostated ultrasonic bath at 20°C for 10 min. Figure 1(a) is the surface of an EP–PP binary blend which will be used as a reference. It is seen that EP elastomer particles were etched by xylene and appear as dark holes on the cut surface. Figure 1(b) shows the surface of the PP/EP/talc hybrid with a separate particle microstructure. It is seen that talc (brighter sheet) and elastomer (dark hole) are separated in the PP matrix. There are no gaps between talc particles and PP. Figure 1(c) shows the PP–EP–talc hybrid with a core–shell microstructure. It is seen that the size and shape of the dark holes were significantly different from the binary blend and the hybrid with a separate particle microstructure. This is expected because EP rubber is concentrated at the interface between the PP and talc in the hybrid with a core–shell microstructure. When the rubber was removed, some of the talc will also be removed. Further observation shows that the shape of the elastomer in the hybrid with a separate particle microstructure can be considered spherical, which is similar to a PP/EP binary blend. The shape of EP elastomer holes in the PP/EP/talc hybrid with the core–shell microstructure is random because the shape depends on the shape of the talc particles.

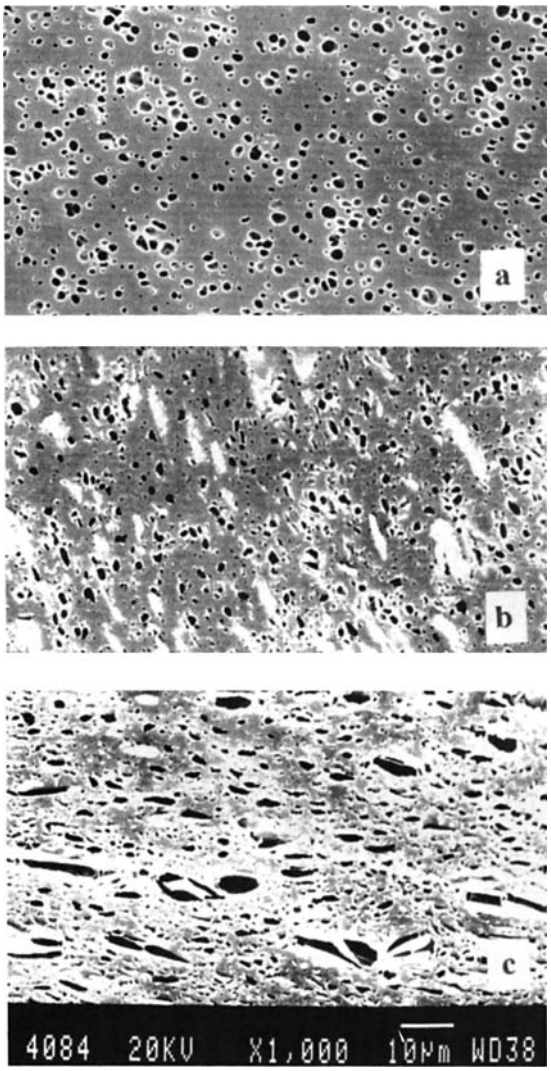

Figure 1 SEM micrographs of cut and etched surfaces: (a) PP/EP binary blend; (b) PP/EP/talc hybrid with separated microstructure; (c) PP/EP/talc hybrid with core–shell microstructure.

Similar morphologies of the different microstructures can also be observed in PP/EP/$CaCO_3$ hybrids (see Fig. 2). Figure 2(a) shows the surface of the PP/EP/$CaCO_3$ hybrid with separated particle microstructure. It is seen that $CaCO_3$ particles can be clearly identified and they are separated from the elastomer particles. It has been noticed that some of the $CaCO_3$ particles were also removed during the etching process because of the poor adhesion between $CaCO_3$ and PP matrix; this resulted in a rough surface. Figure 2(b) shows a PP/ma-EP/$CaCO_3$ hybrid with a core–shell microstructure. It is seen that both the elastomer and $CaCO_3$ particles have been removed from the surface. The shape of rubber particles remained spherical and larger rubber particles covered more than one $CaCO_3$ particle.

Morphologies of PP/EP/PA hybrids were studied from their fracture surfaces. Figure 3 shows the fracture surfaces of PP/EP/nylon-12 hybrids with different microstructures. Figure 3(a) is the fracture surface of the PP 80/EP 20/nylon-12 10 hybrid with a separate particle microstructure. It is seen that the nylon-12 particles were separated from the matrix. Some larger particles of nylon-12 were observed because of its poor dispersion. Elastic deformation was observed, which was contributed by EP particles in the PP matrix. Figure 3(b) is the fracture surface of the PP 80/ma-EP 20/nylon-12 10 hybrid with a core–shell microstructure. When the EP rubber was interspersed between nylon-12 and the PP matrix to form a core–shell microstructure, the dispersion of the nylon-12 particles in the PP matrix was improved significantly. It is seen from Figure 3(b) that elastic deformation appeared on the interface between nylon-12 particles and the PP matrix to form fibrils. The observation of fibrils not only confirmed the microstructure difference but can also be used to explain the improvement in toughness by the

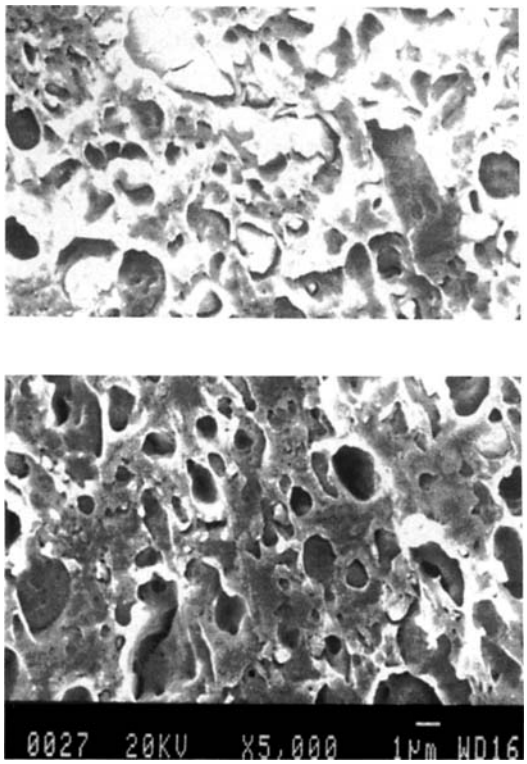

Figure 2 SEM micrographs of cut and etched surfaces of PP/EP/$CaCO_3$ hybrid with different microstructures: (a) separated microstructure; (b) core–shell microstructure.

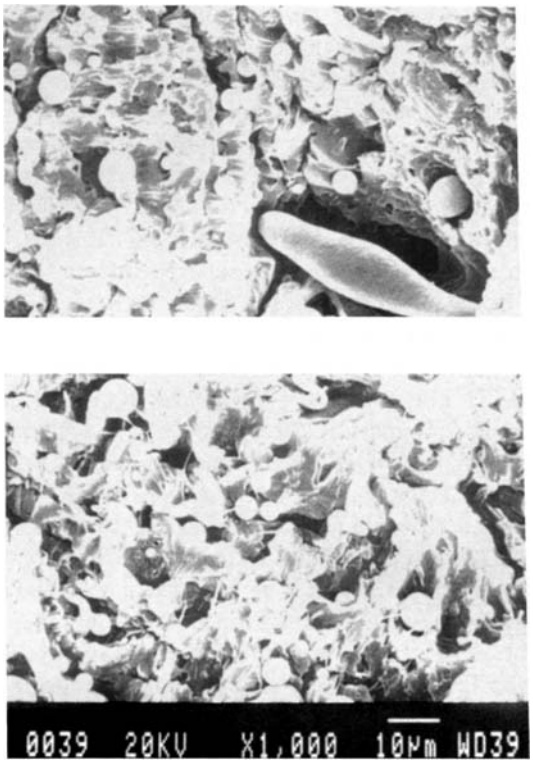

Figure 3 SEM micrographs of fracture surfaces: (a) PP/EP/nylon-12 hybrid with separated microstructure; (b) PP/ma-EP/nylon-12 hybrid with core–shell microstructure.

core–shell microstructure. It is well known that PP and polyamide are immiscible and incompatible because their interfacial adhesion is weak; this results in their poor dispersion. In this particular blend, PP is a hydrophobic nonpolar polymer, while nylon-12 is a hydrophilic polar polymer. Maleic anhydride-grafted EP rubber cannot only act as a toughening agent, but also as a compatibilizer. The compatibilization is considered to occur through a chemical bond between the anhydride on the compatibilizer chain and the nylon amine end group, forming amide and imide groups.[2] Previous work has confirmed the formation of a graft copolymer through reaction of the anhydride with the nylon end group using solvent extraction.[2,3] Similarly, maleated copolymer (PP-ma-*g*-PEO),[4] and acrylic acid-functionalized PP[5] can also be used as compatibilizers for PP/nylon blends.

The results from DSC have confirmed that there is a difference in the microstructures. Figure 4 shows DSC curves for crystallization of different microstructures in PP/SEBS/talc hybrids. It is seen that for a certain formulation the crystallization temperature of a separated microstructure is higher than that of a core–shell microstructure. Similar results have been found in other PP/rubber/filler hybrids (see Table I). Optical microscopy with image analysis has shown that in the core–shell microstructure the overall crystallization growth was decreased, possibly due to a reduction in nucleation. This is expected because in the core–shell microstructure the area of interface between filler and PP is decreased by the elastomer interlayer. The surface of a filler can usually act as a nucleating center and the effect of filler on the nucleation is much stronger than that of the elastomer.[6]

It is well known that the crystallization enthalpy, ΔH_c, is a quantity proportional to the heat of crystallization of a given sample and, thus, to its degree of crystallinity. Since the measurements on all of

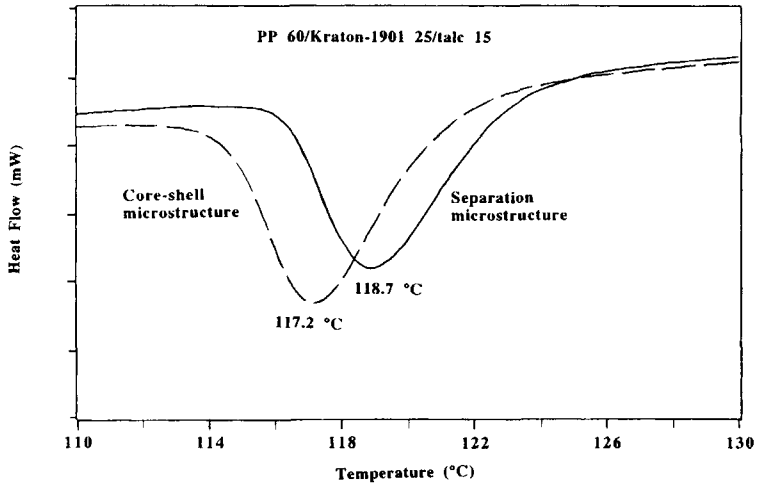

Figure 4 DSC curves of crystallization of PP/SEBS/talc hybrid with different microstructures.

Table I Thermal Behavior of Different Microstructures

Materials	Microstructure	Peak	Onset	ΔH
PP60/SEBS25/talc 15	Separation	118.69	123.29	51.55
PP60/SEBS25/talc 15	Core–shell	117.19	121.29	51.56
PP55/EP30/talc 15	Separation	117.71	121.05	46.50
PP55/EP30/talc 15	Core–shell	114.70	118.46	46.10

the samples were performed under identical instrument settings, the variations in ΔH_c may be taken to represent the variations in crystallinity. The results show that crystallinity was not affected significantly by the distribution of the components. This is expected because both filler and elastomer affect mainly the crystallization growth rate but not the crystallinity.

DSC has also shown the improvement of compatibility between PP and nylon-12 after addition of the ma-EP elastomer in the PP/ma-EP/nylon-12 hybrids. Compatibility between polymers can be characterized by their crystallization temperature difference, ΔT. Table II gives the effect of the added component on the crystallization of PP and nylon-12. It is seen that the ΔT of nylon-12 and the PP crystallization temperature is 41.73°C. Addition of EP slightly decreased the crystallization temperature of both nylon-12 and PP, but did not affect the ΔT. The slight change of crystallization can be explained by a reduction of nuclei in both nylon-12 and PP. To prove this assumption, 10% wt of $CaCO_3$ was added to the PP/nylon-12 blends as a nucleating agent. It was found that $CaCO_3$ only changed the crystallization temperature but not ΔT, which was similar to the effect of EP. When ma-EP was used in the hybrids, the situation was different: The crystallization temperature of nylon-12 decreased while the PP crystallization temperature increased; ΔT was decreased to 37.42°C. The compatibility of PP and nylon-12 was clearly improved, which corresponded with the SEM observation.

Examination of a fracture surface of PP/EP/talc hybrids shows clearly the difference between separation and core–shell microstructures. Figure 5(a) shows an SEM picture of the impact fracture surfaces of a PP/EP/talc hybrid. It is seen that there is a poor interfacial adhesion between the talc and the PP matrix: talc particles show a distinct separation from the matrix. This is expected because a poor interface between PP and the talc has been observed previously. Figure 5(b) shows an SEM micrograph of the fracture surface of a PP/ma-EP/talc hybrid with a core–shell microstructure. It is seen that the surface is cleaner and the talc particles are partly embedded in the polymer. Some elastic deformation around the talc was observed. The interfacial improvement for the core–shell microstructure is likely contributed by the modified elastomer.

On the basis of above experimental results, Figure 6 shows a schematic representation of morphologies of PP/elastomer/filler hybrids with different microstructures. The morphology of the separated microstructure is rather simple: Each additional component was distributed separately in the PP matrix and elastomer particles kept the same shape and size as in the PP/elastomer binary blend. The morphology of the core–shell microstructure was dependent on the shape and size of the filler particles. If the size of the filler particles was similar to or smaller than the size of the elastomer particles, such as $CaCO_3$, it is possible to form multiple cores and the shape of the elastomer particles will still tend to be spherical because of the surface tension between the elastomer and the PP matrix. If the particle size of the mineral filler was larger than the size of the elastomer particles, the maleic anhydride-modified

Table II Effect of Additional Components on the Crystallization of PP and Nylon-12

Materials	$T_{\text{nylon-12}}$	T_{PP}	ΔT
PP 50/nylon-12 50	152.10	110.37	41.73
(PP 50/nylon-12 50) 80/EP 20	151.64	110.02	41.62
(PP 50/nylon-12 50) 80/EX 20	150.71	113.29	37.42
(PP 50/nylon-12 50) 90/$CaCO_3$ 10	154.89	113.74	41.66

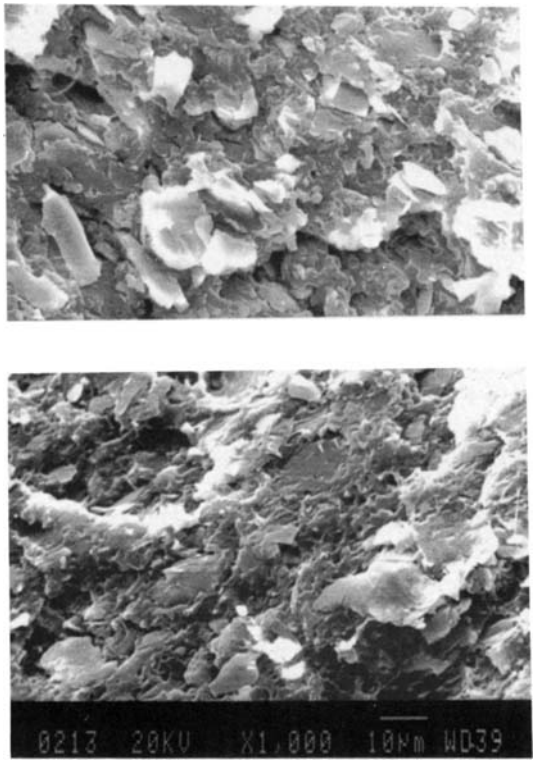

Figure 5 SEM micrographs of fracture surfaces of PP/EP/talc hybrid: (a) separated microstructure; (b) core–shell microstructure.

elastomer tended to form an interlayer between the filler and the PP matrix. The shape of the elastomer shell was dependent on the shape of the filler and the shell could be imperfect.

When polyamide (nylon-12) was used as a filler in the PP/ma-EP/nylon-12 hybrid, the nylon-12 appeared as spherical particles and was surrounded by the ma-EP elastomer. Theoretically, there are two possible microstructures for the particles of nylon-12 with ma-EP: One is when nylon-12 and ma-EP are mixed together to form binary blend particles. The other is when ma-EP forms a shell around the nylon-12 particles. If the microstructure of the particles is of the former case, it will appear that the volume fraction of nylon-12 increases because the total volume fraction of the particles is increased. This was not observed through SEM observation. A possible explanation is that the propylene units in the ethylene–propylene copolymer tended to prefer the PP matrix which resulted in preventing all the EP elastomer from simply mixing with nylon-12. Furthermore, in the maleic anhydride-grafted ethylene–propylene copolymer, the maleic anhydride group is more likely grafted onto the ethylene units than onto the propylene units because the propylene

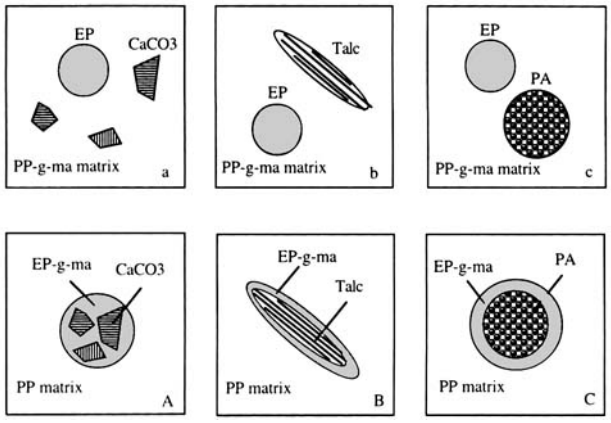

Figure 6 Schematic representation of different microstructures of elastomer-modified and filled PP: (a–c) show a separated microstructure; (A–C) show a representative core–shell microstructure (in which EP is the elastomer and PA is the polyamide).

units preferentially undergo scission when hydrogen abstraction leaves a radical on the chain. The maleic anhydride-grafted ethylene units will have chemical bonds to the polyamide, while the propylene units, without grafting, will have poor miscibility with the polyamide, which leads to formation of a core–shell microstructure.

Morphologies of the various hybrids were also studied quantitatively by digital image processing and analysis. Figure 7 shows the measured EP rubber particle density in a PP 80/EP 20 binary blend and PP 80/EP 20/talc 10 hybrid with different microstructures. It is seen that there is no significant difference between the particle densities. Figure 8 shows the measured area fraction for EP rubber particles. It is seen that there is no significant dif-

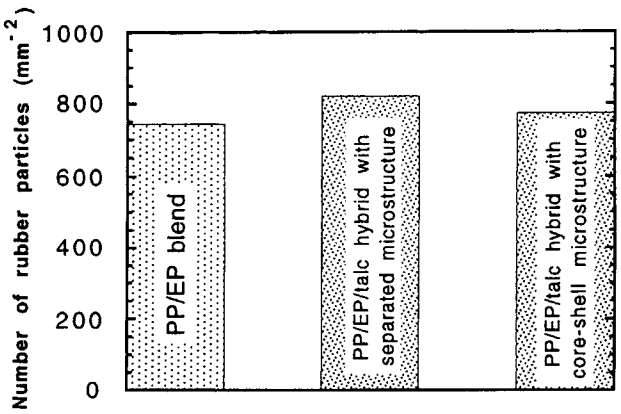

Figure 7 Measured EP elastomer particle density in PP 80/EP 20 binary blend and PP 80/EP 20/talc 10 hybrid with different microstructures.

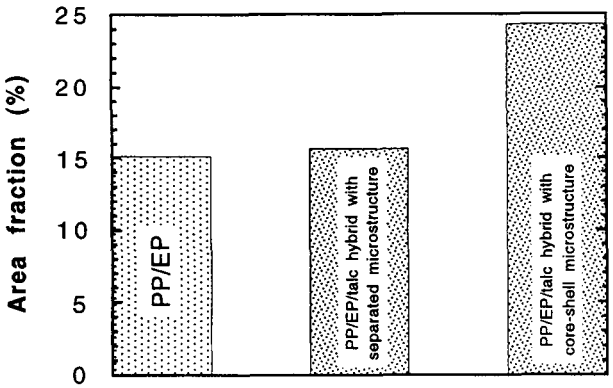

Figure 8 Measured area fraction of EP elastomer particles in PP 80/EP 20 binary blend and PP 80/EP 20/talc 10 hybrid with different microstructures.

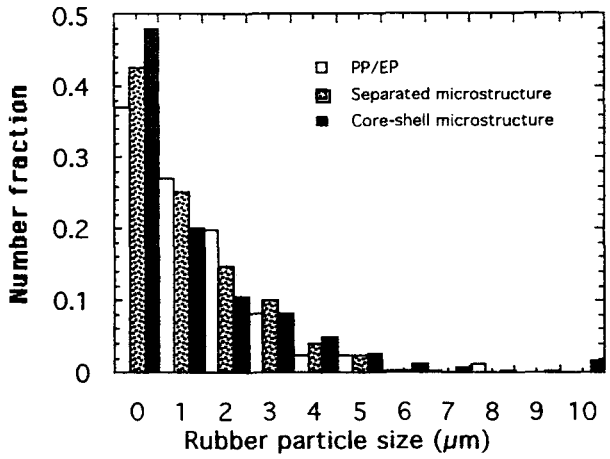

Figure 9 Number distribution of measured EP elastomer particles in PP 80/EP 20 binary blend and PP 80/EP 20/talc 10 hybrid with different microstructures.

ference between PP 80/EP 20 binary blend and PP 80/EP 20/talc 10 hybrid with different microstructures, but the area fraction in the PP 80/EP 20/talc 10 hybrid with a core–shell microstructure increased significantly. This means that a core–shell microstructure increases the elastomer "volume fraction." This is expected because the filler core increased the measured elastomer content. It has been noticed that the measured area fractions of elastomer in both the PP/EP binary blend and the PP/EP/filler hybrid with a separated microstructure were lower than the actual amount present. The reason for this can be explained by the limitation of a two-dimensional measurement on a surface[7]: since radii of spheres cut at most cross sections are smaller than the actual radii of the spheres.

Figure 9 shows the number distribution of measured EP elastomer particles in the PP 80/EP 20 binary blend and PP 80/EP 20/talc 10 hybrid with different microstructures. It is seen that all the shapes in the distribution are similar: The number fraction decreased as the size increased. About 40–50% of the particles are smaller than 1 μm. It should be pointed out that the cumulative frequency of the particle sizes up to 10 μm in the binary blend and the hybrid with the separated microstructure was nearly 100%, and in the hybrid with the core–shell microstructure, it was about 85%. That means there is about 15% of EP particles in the hybrid with core–shell microstructures larger than 10 μm which were not shown in this figure.

Figure 10 shows the measured area distribution of EP rubber particles in the PP 80/EP 20 binary blend and the PP 80/EP 20/talc 10 hybrid with different microstructures. It is seen that the area distribution in the PP 80/EP 20/talc 10 hybrid with a core–shell microstructure changed significantly: The area fraction of small particle sizes decreased and the area fraction of large particle sizes increased. Further observation showed that the area fraction of the particles with sizes smaller than 5 μm in the binary and the hybrid with the separated microstructure were about 92 and 98%, respectively; but in the hybrid with the core–shell microstructure, it was only about 54%. The results corresponded with the measured area fraction of the elastomer in the materials (see Fig. 7). That means that there is no significant difference between the particle densities, but the elastomer area fraction in the PP 80/EP 20/talc 10 hybrid with the core–shell microstructure increased because the elastomer particle size increased. These results can be used as one of the rea-

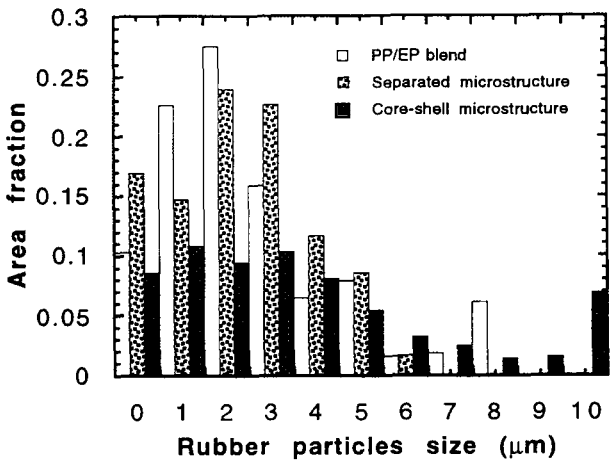

Figure 10 Area distribution of measured EP elastomer particles in PP 80/EP 20 binary blend and PP 80/EP 20/talc 10 hybrid with different microstructures.

sons to explain the increase in toughness because the particle distance is inversely proportional to the particle size if the particle densities are the same.

CONCLUSION

The microtome sampling technique with SEM and optical microscopy is a useful tool to study the microstructures of PP/elastomer/filler hybrids. The difference between the separated microstructure and the core–shell microstructure was clearly observed by SEM through microtomed and etched surfaces. The fracture surfaces were different for the same compositions with different microstructures. In the core–shell microstructure of the PP/EP/talc hybrid, the talc particles are partly embedded in the elastomer. Some plastic deformation around the talc was observed. In the core–shell microstructure of the PP/EP/nylon-12 hybrid, elastic deformation appeared on the interface between the nylon-12 particles and the EP shell to form fibrils. The microstructures observed by SEM corresponded to the designed microstructures.

A quantitative optical microscopy study of morphologies showed that elastomer particles in the PP/elastomer binary blend and the PP/elastomer/filler hybrid with a separated microstructure were similar. Elastomer particle size and particle-size distribution in the PP/elastomer/filler hybrid were significantly different from the PP/elastomer binary blend and the PP/elastomer/filler hybrid with a separated microstructure. There was no significant difference between the particle densities, but the elastomer area fraction in the PP 80/EP 20/talc 10 hybrid with a core–shell microstructure increased significantly because the elastomer particle size increased. These results can be used as one of the reasons to explain the increase in toughness.

This project was funded by the CRC for Polymer Blends in collaboration with ICI Australia Pty Ltd. Thanks are given to Dr. A. McKee for useful suggestions.

REFERENCES

1. Y. Long and R. A. Shanks, *J. Appl. Polym. Sci.*, to appear.
2. F. Ide and A. Hasegawa, *J. Appl. Polym. Sci.*, **18,** 963 (1974).
3. S. Hosoda, K. Kojima, Y. Kanda, and M. Aoyagi, *Polym. Networks Blends,* **1,** 51 (1991).
4. T. Tang, H. Li, and B. Huang, *Macromol. Chem. Phys.*, **195,** 2931 (1994).
5. Z. Liang and H. L. Williams, *J. Appl. Polym. Sci.*, **44,** 699 (1992).
6. Y. Long, Z. H. Stachurski, and R. A. Shanks, *Mater. Forum,* **16,** 173 (1992).
7. A. Galeski, *Int. Polym. Sci. Tech.*, **8,** T/28 (1980).

Received November 21, 1995
Accepted May 10, 1996